Kufa Journal of Engineering
Vol. 16, No. 1, January 2025, P.P. 200-213
Article history: Received 4 June 2024, last revised 8 August 2024, accepted 11 August 2024

THE EFFECT OF ZIRCONIUM ADDITIVES ON PROPERTIES OF (Cu22%Zn4%Al) SHAPE MEMORY ALLOY

Zainab Hassan[1] and Ekbal Mohammed Saeed[2]

[1] Metallurgical Engineering Department , collage of Materials Engineering , University of Babylon,Babal, Iraq, Email: zainabhchallab@gmail.com.

[2] Metallurgical Engineering Department / collage of Materials Engineering / University of Babylon, Iraq, Email: Mat.ekbal.moh@uobabylon.edu.iq.

https://doi.org/10.30572/2018/KJE/160112

ABSTRACT

Shape memory alloys (SMAs) are one of the most important types of smart materials. It define as the materials that can undergo large pseudo elastic deformations while having the ability to recover to their original shape once subjected to a memory stimuli such as a specific temperature ,stress ,or strain. This study examines the effects of varying Zirconium (Zr) additive amounts on the microstructure, mechanical, and shape memory effect for all specimens of Cu-Zn-Al SMAs. Powder metallurgy was used to create Cu–22%Zn–4%Al SMAs, both base and with the inclusion of 0.2 and 0.4 weight percent Zr. 650MPa compact pressure was used to create the alloys after the particles had been mixed for five hours. The alloys underwent a three-step sintering procedure in a vacuum tube furnace for one hour at 350 ˚C, then for one hour at 550 ˚C, and for two hours at 850 ˚C. To characterise the microstructural and phase characteristics of alloys, both with and without Zr additions, XRD diffraction analyses, optical microscopy (OM), and scanning electron microscopy (SEM) were performed. With differential scanning calorimetry, the transition temperatures of all alloys were determined (DSC).As well as the shape memory effect test (SME) was measured. Results confirmed that all alloys compositions were found to include the predominant (Cu_5Zn_8) phase, as proven by XRD and microstructural investigation. The Zr addition dramatically lowered the transition temperatures, according to the transformation temperature data. Hardness experiments reveal that alloys' hardness and volume losses were enhanced by adding up to 0.4% weight percent of Zr reached to (64.8%) and (0.3909)mm3 respectively compared to base alloy.

KEYWORDS

Smart materials; Shape Memory Effect; Transformation temperature; Powder Metallurgy; Mechanical properties.

1. INTRODUCATION

Shape memory alloys (SMAs) are a class of materials that, when exposed to specific stimuli involving changes in temperature, mechanical, electrical, chemical, light, and magnetic fields, remember their prior form (Dasgupta,2014). Out of these material SMAs haves widely used due to its relatively higher value of specific strength, corrosion resistance , wears resistance , fatigue properties and good actuation response (Guerioune et al,2008). Currently, Ni-Ti alloys and Cu-based alloys are the most studied alloys which offer SME. (SMA) can be framed between the new functional materials, which can be used mainly in actuators, microcontrollers and sensors (Jani et al,2014). They are distinct from other common alloys due to their two unique functional properties: (i) shape memory effect (SME), which is the capacity to regain its original shape following deformation, and (ii) super elasticity (SE), also known as pseudo elasticity, which is the capacity to recover a significant non-linear strain during loading and unloading (Otsuka et al,1999; Otsuka et al,1998). The thermo elastic martensitic transformation, a unique class of non-diffusional solid state phase transformation that is a reversible transition with modest volume change and low hysteresis, is responsible for both qualities. The majority of SMAs fall into one of three main groups among the systems of alloys that exhibit SME and SE: Cu-based SMA (Cu–Al–Ni, Cu–Zn–Al, Cu–Al–Mn, etc.); those incorporating NiTi and Fe-based SMA (Fe–Mn–Si, Fi–Ni–Co–Ti, etc.). Due to their superior functional qualities, the first two groupings are utilized in engineering applications more frequently than the latter. Nevertheless, because of the material's high melting temperature and high cost, the manufacturing procedure for NiTi-based SMAs is complicated, even if they have excellent SME, SE, high biocompatibility, and high corrosion resistance (Wu S et al,2019; Mazzer,2022). Cu-based shape memory alloys have a lower melting point than NiTi-based SMAs, which have a wider transformation temperature range and better SME. As a result, manufacturing costs are lower and the process is less complicated (Malinin V et al,2018; Yu C et al,2018). Nevertheless, the brittle inter granular fracture that polycrystalline Cu-based SMA are prone to restricts their practical applicability. Because the incompatibility of plastic and elastic deformations between the grains causes stress accumulation in the grain borders and triple junctions, high elastic anisotropy is the primary cause of it (Y. Chen et al, 2011; S.M. Ueland et al, 2012). Numerous attempts have been made to enhance the mechanical properties of the polycrystalline Cu-based SMA, using various processing techniques (S.K. Vajpai et al, 2013; R.D. Cava, 2014) and compositional modifications including the addition of alloying metals for precipitate formation or grain refining (Alaneme,2018). (Al-Hassani et al,2017) used powder metallurgy technology to make the alloy (Cu-(15, 20, 25, 30, 35, 40 wt %Zn) -6wt.%Al)

and a fixed proportion of Al quantity of 6.wt%Al to evaluate the impact of these components on SMA.Then, replace the aluminium, by elements (Si, Sn, and Ni) was added at a predetermined weight percent of 6. Result shows alloying element addition has no influence on the current phases at these ratios. As zinc increase, the intermetallic CuZn combination which affects hardness became more prevalent. (Zainab Salim et.al ,2021) Cu-21%Zn-6%Al SMA's microstructure attributes were investigated in relation to the effects of Ag nanoparticle addition at various percentages (0.12, 0.15, 0.25, and 0.35 wt.%). The particle size was refined as the amount of Ag nanoparticles supplied increased from 0 to 0.25 weight percent, reducing from 1551 µmto 212 µm with an 86.32 weight percent reduction.

This study aims to investigate The effect of Zr on Cu 22%Zn4%Al shape memory alloy on properties and investigate their surface morphology ,phase composition ,wear resistance with different load and Shape Memory Properties.

2. EXPERIMENTAL WORK

2.1. Materials

The experimental work included preparation and characterization for all specimens. First step was prepared powders of Copper (Cu), Zinc(Zn) , Aluminum(Al) and Zirconium (Zr)of 99.9% purity were used as raw materials to prepare the alloy specimens of the present study. The particle size of the powders was analyzed via (the better size 2000, laser particles size analyzer). The tests were carried out at the University of Babylon/Colleges of Materials Engs. /Ceramics and Buildings Materials Labs. Table 1 shows the particle size and the supplier of each powder. The test report of particle size analysis is shown in Fig. 2.

Table 1. The partical size and the supplier of the used powders

Material (Powder)	Average Particle Size (µm)	Source
Cu	54.14	Changsha Xinkang Advanced Material Co., Ltd.
Zn	16.49	Changsha Xinkang Advanced Material Co., Ltd.
Al	18.66	Changsha Xinkang Advanced Material Co., Ltd.
Zr	6.162	Changsha Xinkang Advanced Material Co., Ltd.

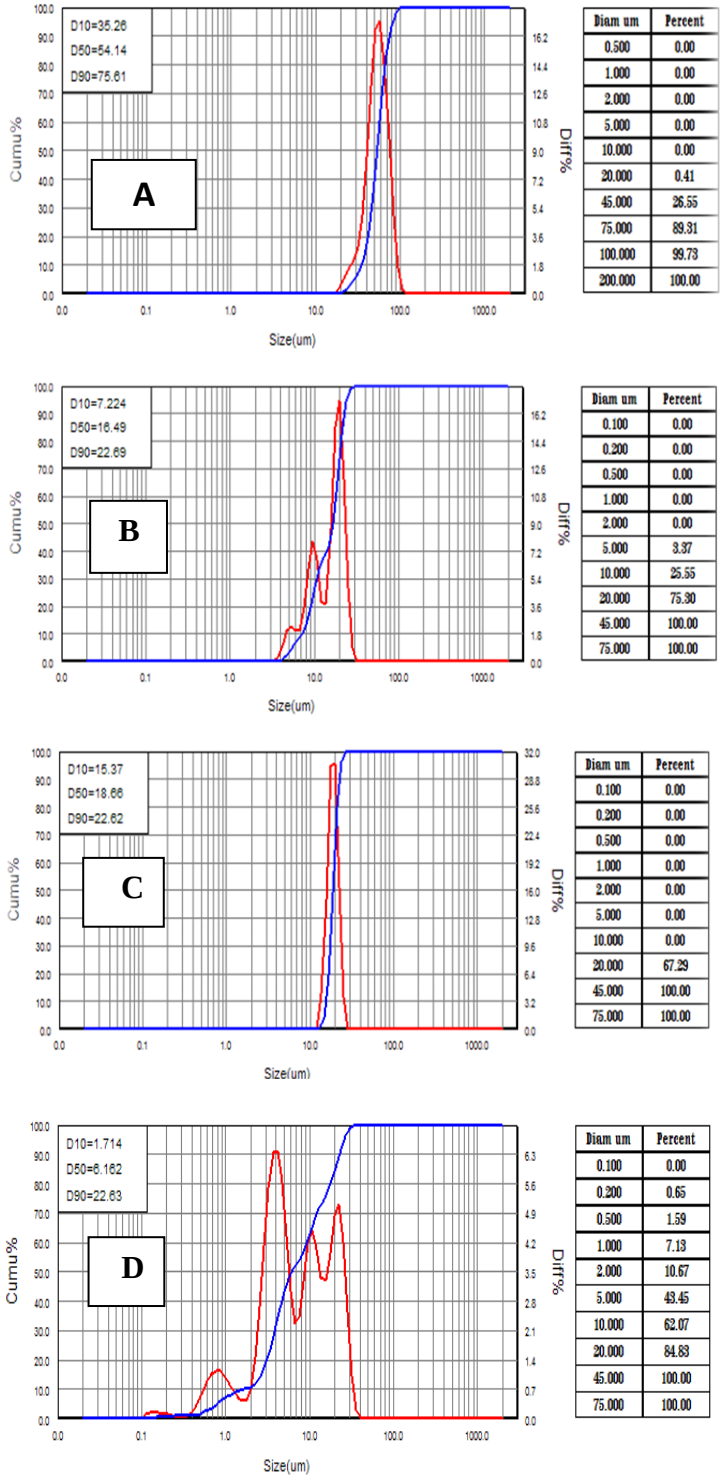

Fig. 1 Test Report of Particle Size Analysis; (A) Copper; (B) Zn ; (C)Al (D)Zr

2.2. Alloy Preparation of Cu-Zn-Al SMA

In the process of manufacturing the specimens using powder metallurgy, Cu-22%Zn-4%Al-XZr (x=0.2%, 0.4%)because of the preferred content of Zr is 0.001 to 1 weight% (Ishida,2002), is the primary mixture utilized. After that, the weighted powder combination was mixed for

five hours in order to obtain a fine and consistent dispersion of particles powder. The cold uniaxial pressing cylindrical die was used to prepare specimens with dimensions (12 mm in diameter and 6mm in thickness) as a shown in Fig.2a. The compact pressure was found to be 650 MPa has been used as an optimal compressive stress that give higher green density and lower green porosity. After that, the material was sintered in inert gas (argon) for one hour at 350 ˚C, then for one hour at 550˚ C, and for two hours at 850 ˚C.The specimens were then allowed to cool to room temperature in the furnace type (MIT- GSL1600X)as a shown in Fig.2b.To stabilize β-phase structure, Quenching heat treatment has been done for all specimens at 850^{o} C for 1h rafter that rapid cooling carried out by immersing in a cooling medium cold water(20^{o}C) (Ishida,2002).Table 2 provides details on the specimen code and composition used in this experiment.

Table 2. prepared specimens in the present study.

Alloy Code	Chemical Composition (wt) %
(base)	Cu-22%Zn-4%Al
A	Cu-22%Zn-4%Al-0.2%Zr
B	Cu-22%Zn-4%Al-0.4%Zr

Fig 2: a- Type of Prepared Specimens **b- Vacuum Tube Furnace**

2.3. Inspection of alloy.

SiC paper grits sized (250, 400, 600, 800, 1000, 1200, 1500, and 2000) used in the wet grinding and polished with diamond paste; and etched in a room-temperature solution of (10 mLHCl+5 gFeCl3+H2O) according to ASTM E407 - 07 (The specification number savailable in the references). The specimen was washed and dried using distilled water and an electric dryer following etching. A light optical microscope of the Belphoptic type was used to view and study the specimens' microstructure, and a JEOL-JSM scanning electron microscope (SEM) was used to look at the samples' microstructure up close. We used an X-ray diffract meter (XRD) (model: X-Pert Pro) to study the base's phases. In the XRD studies, CuKa radiation operating at 40 KV

and 7 mA was used as the X-ray source. The samples were scanned in a θ range from 30 to 80, and elemental composition was investigated using energy dispersive spectroscopy (EDS).

2.4. Mechanical Tests

Sintered specimens were prepared carefully for this test. Universal macro hardness tester type (Wilson Hard REICHERTER UH 250) was used. The tests were conducted according to **ASTM (E10-15a)** using a ball of 2.5 mm diameter with a load of 15 kg for duration of 10sec.

The wear testing was conducted according to **G99-04 ASTM**. The test was performed at room temperature, utilizing a constant load (3,6,10) N and a constant radius of 2 mm with a rotational speed of 250 rpm. The test started after the specimen was weighed on a sensitive balance to an accuracy of 0.0001. After (5, 10, 15, 20 ,25min). The relation between weight loss and time was drawn to calculate the wear rate for all tested specimens.

$$\text{Volume loss}(mm^3) = \frac{weight\ loss(g)}{density\ (\frac{g}{cm^3})} * 1000 \quad (1)$$

weight loss (g)=weight loss after (5,10,15,20,25 min).

Density g/cm³=theoretical density of elements

2.5. Shape Memory Properties.

Shape memory properties has been studied by shape memory effect test and transition temperatures test

2.5.1. Shape Memory Effect Test

Based on compression tests, the shape memory effect was ascertained as follows (M. H. Wu,1990) :

$$\text{Where: Shape memory effect(SME \%)} = \frac{d_b - d_a}{d_b} * 100\% \quad (2)$$

d_b=diameter of impression in mm before heat treatment.

da= diameter of impression in mm after heat treatment.

2.5.2. Differential Scanning Calorimeter (DSC) Analysis

Differential Scanning Calorimeter (DSC) analysis has been done in order to estimate the transformation temperatures for specimens for the forward transformations to determine the A**s** (austenite start temp.) and A**f** (austenite finish temp.) and use these temperatures for the shape memory effect test**.** This test is carried out in furnace with temperatures ranging from 20-360°C and a heating rate of 5˚C/ min. These are the specifications of the furnace used.

3. RESULTS AND DISCUSSIONS .

Fig. 3(a) shows base alloy, obviously there a coarse grains or roughness. this is expect, because ,it represents one of the characteristic of this alloy without any improvements or additions which

have significant impact on the properties while for (A) alloy the grain became fine with (0.2%)Zr alloying element addition and became finer for B alloy when percentage of Zr reach (0.4%) respectively as a shown in Fig. 3(b,c) (Narasimha , 2019) .

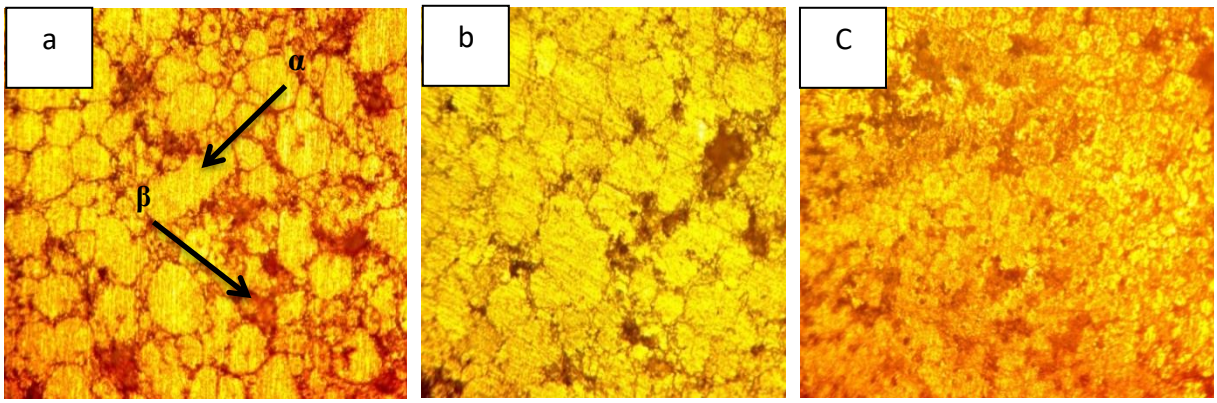

Fig.3. Optical Microscope Image(20X): (a) for Sintered base Alloy, (b) for Sintered A alloy (c) for Sintered B alloy .

X-ray diffraction tests which done for all specimens after the sintering**.** For base alloy in Fig.(4a), it can be seen all phases appeared for this alloy:Cu_5Zn_8 intermetallic compound (quenching mainly producesβ phase) ,AlCu (γ-cubic phase),Cu_9Al_4(γ_2 –solid solution),$CuAl_2$(tetragonal superstructure) and Cu,Zn pure peaks (Kwarciak,1986). All phases appear at (3-5) position in X-ray chart .while Fig.(4b) after adding (0.4%) Zr XRD diffraction for B alloy show no different in results except (Zn_2Zr_3) appear (intermetallic compound) (Wang,2010). this intermetallic compound effective strengthening phases.

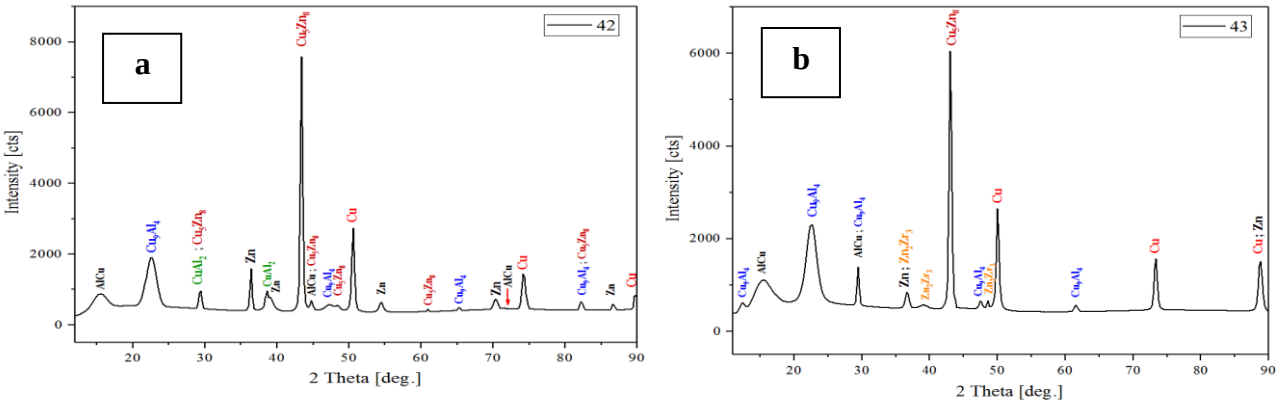

Fig.4. XRD for (a) base alloy (b) XRD for B alloy

In Fig. 5 It is a confirmation of the observations mentioned in the previous paragraph,where the rough structure is clear and the porosity is wide spreads in base alloy as shown in a Fig.5(a). But when the Zr element was added, the picture begain to change , as the grains begein to become finer ,with opportunity for other phases and compounds to appear as it show in x-ray diffraction for (A ,B) specimens as shown in Fig. 5(b, c) respectively (Saha, 2019) .

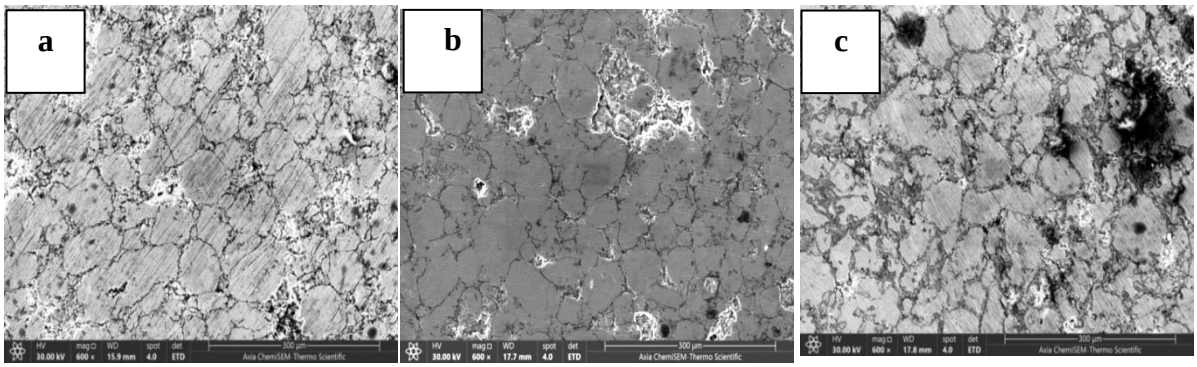

Fig.5. SEM image for (a) base alloy,(b)for A alloy and (c)for B alloy .

The results of Energy dispersive spectroscopy (EDS) that studied and analyzed used to show the chemical composition of all alloys. From tables attached to the Fig. 6(a,b) the percentage of Zn decreases significantly below its theoretical amount (22%) Zn it decrease to 10% for base alloy and 8% for (B) alloy ,this can be attributed to evaporation of Zinc. The evaporation temperature of zinc (907^{o}C) is at normal atmospheric pressure, but this temperature decreases to (330^{o}C) at low pressures 10^{-2}, and this pressure is the pressure of the sintering furnace. Therefore, there will be significant evaporation and a decrease in the percentages of zinc added, and this decrease will certainly affect the properties of the alloy as it is a shape memory alloy and thus It affects the behavior of the SME and the transformation temperatures (Ms, Mf, As, Af) which refers to (martensite start, martensite finish, austenite start and austenite finish) respectively, and this is reflected in the application

Brinell hardness has been presented in Fig. 7 It was found that there was a gradual improvement in the hardness values. The base specimen has a modest value, as one of the characteristics of this alloy is that it has moderate mechanical properties, and this is expected because zinc dissolve usually in copper and form substitution solid solution with copper, and this will certainly generate a somewhat acceptable hardness (Mazzer,2022). As for aluminum, its percentage is small (4%), and according to XRD test, it is a group of intermatallic compounds. Usually, these compounds also add good mechanical properties to copper, but their percentage is small (Ishida,2002). In case of alloying elements(Zr) at ratio (0.2,0.4)%, there is a significant improvement in the hardness values from 40 HB for base alloy, became 59.2 HB with an improvement reached 48% for specimen A and for specimen B the hardness value increased more to (64.8HB), with an improvement reached 51% compared to the base specimen as ashown in Table 3. this is agreement with (Mazzer,2022).

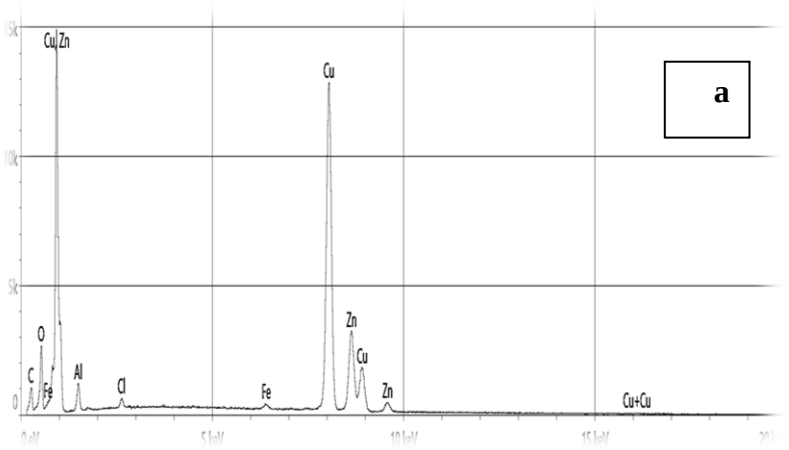

Weight %	Element
8.9	C
11.6	O
3.9	Al
0.6	Cl
0.4	Fe
64.1	Cu
10.4	Zn

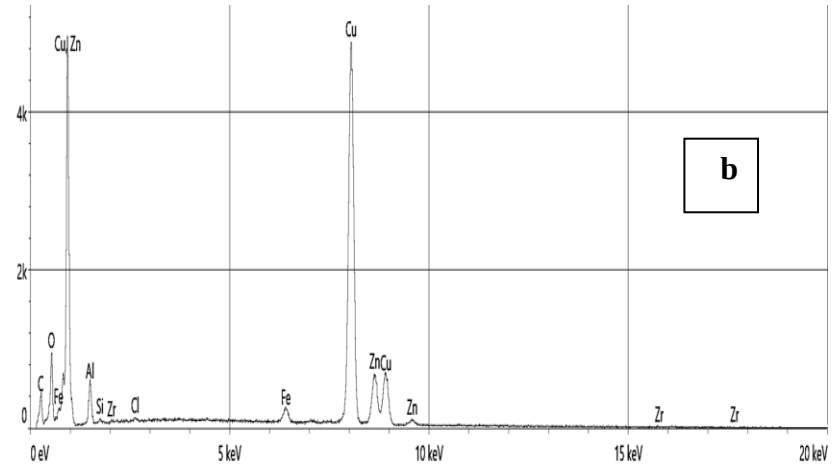

Weight %	Element
11.4	C
11.5	O
5.1	Al
0.3	Si
0.2	Cl
1.2	Fe
61.5	Cu
8.3	Zn
0.4	Zr

Fig.6. EDS for(a)base alloy(b) B alloy.

Table (3):illustrate improving of hardness.

Alloy	Hardness HB	Improving %
Base	40	----
A	59.2	48
B	64.8	51

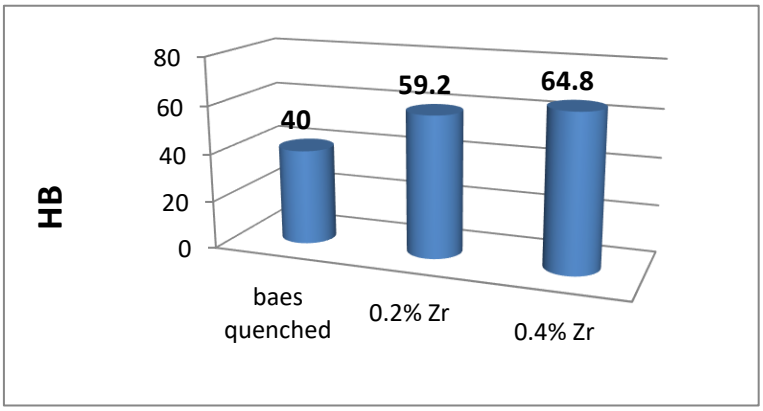

Fig. 7. Hardness for all specimens after sintering

From Fig. 8(a,b and c) can be seen the amount of volume loss (mm3) of (A)and (B) alloys is much less than the base alloy and for all weights (3,6,10)N,.When the load increases, the wear resistance of the specimen surface increases (volume loss decreases) .This is may be discuss as increases hardness , the surface's resistance to wear increases. Wear is directly proportional to hardness and inversely proportional to load. This indicates that the presence of natural proportions of zinc has an effect on wear resistance.in Fig. 8(b,c) It can be seen that with increasing addition of Zr the volume loss decreases. At 0.2%Zr, the volume loss is (0.4465)mm^3 at the load 10N and (0.3909) $mm^3$with the addition of 0.4%Zr at the same load. Because as the percentage of alloying elements increases, the grain size refines, and thus the surface hardness increases and wear resistance increases.

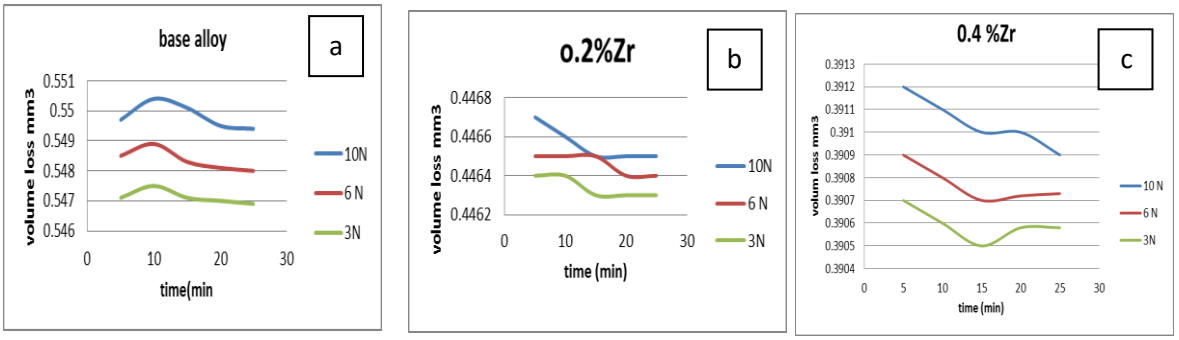

Fig. 8. Volume Loss Vs. Sliding Time for : (a) base Alloy,(b)A alloy (c) B alloy.

Fig. 9 illustrates the results of the DSC test for both the unmodified and Zr-modified Cu-Zn-Al alloys following the sintering process, as indicated by the figures from 7a-c.For the basic alloy (Cu-Zn-Al), it was discovered that the onset temperature (AS) is 284.7ºC and the endset temperature (AF) is 345.9ºC. As we add 0.2 and 0.4 weight percent Zr, we observe that the transformation temperature decreases. However, Fig. 9 illustrates the minimum transformation temperature at 0.4% weight percent Zr, where the transformation temperature starts at 263.34ºC (onset temp.) and ends at 268.64ºC (endset temp.).

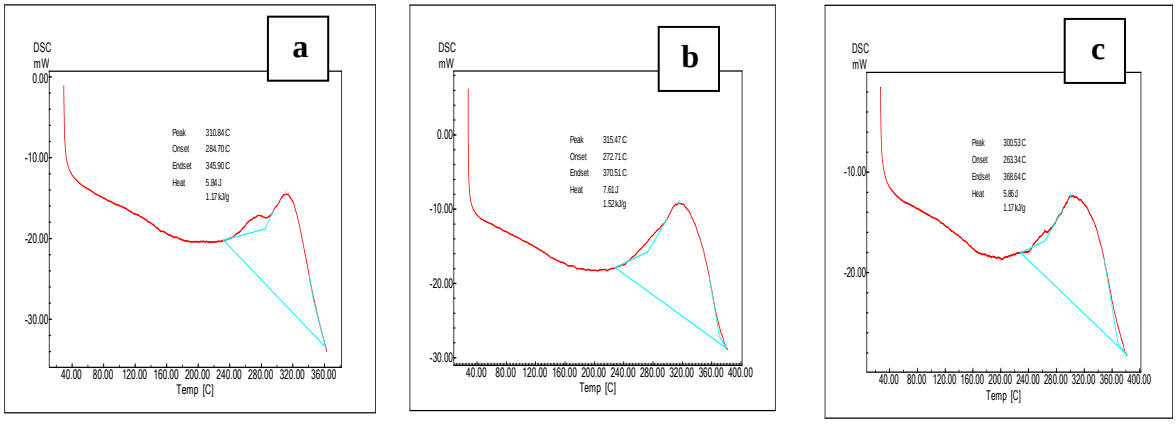

Fig.9. DSC Analysis (a) Base alloy (b)A alloy (c)B alloy.

From Table 4 can be seen that improving in SME for alloy A compare with base alloy. The highest shape memory effect was achieved when the additions was (0.4) wt% of Zr reached to. 3.82%.From the microstructure study it reveals that by refining grain size and with increase in Zn wt.% there is increase in conversion of austenite phase to martensite phase (Lokesh,2022).

Table 4 : shape memory effect and shape recovery for alloys.

Alloy	Alloy composition	d_b	d_a	SME%
Base	Cu+22%Zn+4%Al	0.7018	0.6893	1.82
A	Cu+22%Zn+4%Al+0.2%Zr	0.6110	0.5734	6.153
B	Cu+22%Zn+4%Al+0.4%Zr	0.5719	0.5500	3.82

4. CONCLUSION

This alloy (CuZnAl) SMA suffer moderate properties hardness,wear resistance due to grain growth. In this study, the effect of adding alloying element has been done (0.2% -0.4%) zirconium was studied, which showed positive results on the alloy's mechanical properties and shape memory properties, itcan be summarized as follows:

* Adding the element has an effect in refining the particle size of the alloy, and this effect increases with the increase in the percentage of the added element (0.2%, 0.4%), and it has an effect an improving in hardness reached 59.2 for 0.2%Zr and 64.8 for 0.4%Zr respectively compared with base alloy. There is also a significant improvement in volume loss for all weights (3,6,10)N with increasing weight and time, this can be attributed to reffing in microstructure. The austenite transition temperature value of B (0.4% Zr) alloy was found to be lower than base alloy, while for SME the results show the B alloy has higher SME reached to(6.153)%.

ACKNOWLEDGMENTS

The authors wish to acknowledge the entire staff of materials engineering colleges and universities in Babylon /Iraq for their extended help during experimental activities.

5. REFERENCES

Abd Alhassan, Z. S., & Jabbar, M. A. (2021),' Effect of Ag Nanoparticles Addition on the Microstructure of Cu-21% Zn-6% Al Shape Memory Alloys', *Basrah Journal for Engineering Sciences*, *21*(3).

Alaneme, K. K., & Umar, S. (2018). Mechanical behaviour and damping properties of Ni modified Cu–Zn–Al shape memory alloys. *Journal of Science: Advanced Materials and Devices*, *3*(3), 371-379.

Al-Hassani, E. S., Ali, A. H., & Hatem, S. T. (2017), 'Investigation of corrosion behavior for copper-based shape memory alloys in different media', *Engineering and Technology Journal*, *35*(6A), 578-586.

ASTM E407 - 07 (2011) " Standard Practice for Microetching Metals and Alloys" ASTM international .

ASTM, G., et al. Standard test method for wear testing with a pin-on-disk apparatus. ASTM International: West Conshohocken, PA, USA, 2016.

Cava, R. D., Bolfarini, C., Kiminami, C. S., Mazzer, E. M., Botta Filho, W. J., Gargarella, P., & Eckert, J. (2014), 'Spray forming of Cu–11.85 Al–3.2 Ni–3Mn (wt%) shape memory alloy', *Journal of Alloys and Compounds*, *615*, S602-S606.

Chen, Y., & Schuh, C. A. (2011),' Size effects in shape memory alloy microwires", *Acta Materialia*, *59*(2), 537-553.

Dasgupta, R. (2014) 'A look into Cu-based shape memory alloys: Present scenario and future prospects', *Journal of Materials Research*, *29*(16), 1681-1698.

Duerig, T. W., Melton, K. N., & Stöckel, D. W. C. M. (2013), *'Engineering aspects of shape memory alloys*', Butterworth-heinemann.

Guerioune, M., Amiour, Y., Bounour, W., Guellati, O., Benaldjia, A., Amara, A., ... & Vrel, D. (2008), 'SHS of shape memory CuZnAl alloys', *International Journal of Self-Propagating High-Temperature Synthesis*, *17*, 41-48.

Jani, J. M., Leary, M., Subic, A., & Gibson, M. A. (2014),' A review of shape memory alloy research, applications and opportunities', *Materials & Design (1980-2015)*, *56*, 1078-1113.

Otsuka, K., & Ren, X. (1999), 'Recent developments in the research of shape memory alloys', *Intermetallics*, *7*(5), 511-528.

Ishida, K., Kainuma, R., & Sutoh, Y. (2002). *U.S. Patent No. 6,406,566*. Washington, DC: U.S. Patent and Trademark Office.

Kwarciak, J. (1986),'Phase transformations in Cu-Al and Cu-Zn-Al alloys', *Journal of Thermal Analysis and Calorimetry*, *31*(3), 559-566.

Lokesh, N., Mallik, U. S., Shivasiddaramaiaha, A. G., Mohith, T. N., & Praveen, N. (2022), 'Characterization and Evaluation of Shape Memory Effect of Cu-Zn-Al Shape Memory Alloy',*Journal of Mines, Metals and Fuels*, 324-331.

Malinin, V. G., Malinina, N. A., Malinin, G. V., & Malukhina, O. A. (2018, October). 'Development of methods of structural-analytical mesomechanics that take into account the statistical properties of martensitic transformations in materials with shape memory effect', In *IOP Conference Series: Materials Science and Engineering* (Vol. 441, No. 1, p. 012030). IOP Publishing.

Mazzer, E. M., Da Silva, M. R., & Gargarella, P. (2022), 'Revisiting Cu-based shape memory alloys: Recent developments and new perspectives', *Journal of Materials Research*, *37*(1), 162-182.

Narasimha, G. B., & Murigendrappa, S. M. (2019). Effect of zirconium on the properties of polycrystalline Cu-Al-Be shape memory alloy. *Materials Science and Engineering: A*, *755*, 211-219.

Otsuka, K., & Wayman, C. M. (Eds.). (1999), '*Shape memory materials*', Cambridge university press.

Wu, S., Wang, D., Zhang, Z., Li, C., Liu, X., Meng, X., ... & Di, X. (2019),'Mechanical properties of low-transformation-temperature weld metals after low-temperature postweld heat treatment', *Science and Technology of Welding and Joining*, *24*(2), 112-120.

Saha , G., Ghosh, M., Antony, A., & Biswas, K. (2019). Ageing behaviour of Sc-doped Cu–Zn–Al shape memory alloys. *Arabian Journal for Science and Engineering*, *44*, 1569-1581.

Ueland, S. M., & Schuh, C. A. (2012),' Superelasticity and fatigue in oligocrystalline shape memory alloy microwires', *Acta materialia*, *60*(1), 282-292.

Vajpai, S. K., Dube, R. K., & Sangal, S. (2013), 'Application of rapid solidification powder metallurgy processing to prepare Cu–Al–Ni high temperature shape memory alloy strips with high strength and high ductility', *Materials Science and Engineering: A*, *570*, 32-42.

Wang, S., Zhao, Y., Guo, H., Lan, F., & Hou, H. (2018), 'Mechanical and thermal conductivity properties of enhanced phases in Mg-Zn-Zr system from first principles', *Materials*, *11*(10), 2010.

Yu, C., Kang, G., Xie, X., & Rao, W. (2018),' A micromechanical model for the grain size dependent super-elasticity degeneration of NiTi shape memory alloys', *Mechanics of Materials*, *125*, 35-51.